Hydrogenation of 1,5,9-Cyclododecatriene in Fixed-Bed Reactors: Down- vs. Upflow Modes

R. V. Chaudhari, R. Jaganathan, and S. P. Mathew
National Chemical Laboratory, Pune 411 008, India

C. Julcour and H. Delmas
ENSIGC, 18, Chemin de la Loge—31078 Toulouse Cedex 4, France

Performance of trickle-bed and up-flow reactors was studied experimentally and theoretically for an exothermic multistep hydrogenation of 1,5,9-cyclododecatriene (CDT) in n-decane as solvent over 0.5% Pd/alumina catalyst. Intrinsic kinetics was studied in a batch stirred slurry reactor using the powdered catalyst, and a Langmuir-Hinshelwood-type rate model is proposed. Using this rate equation, a trickle-bed-reactor model was developed that incorporates contributions of partial wetting and stagnant liquid holdup, in addition to the external and intraparticle mass transfer for the gas-phase reactant (hydrogen). It was also modified to describe the behavior of the upflow reactor. Experimental data were obtained in both upflow (trickle-bed) and down-flow modes at different liquid velocities, pressures, and inlet feed concentrations at 373–413 K. Reactor performance of the two modes was compared in terms of global hydrogenation rate, CDT conversion, selectivity to cyclododecene and the maximum temperature rise observed in the catalyst bed. The conversions and global hydrogenation rate were significantly higher in a trickle-bed reactor than in the upflow reactor. Similarly, a significant temperature rise in the catalyst bed was observed for the downflow operation compared to the upflow mode, which is explained from wetting characteristics of the catalyst bed. Model predictions for both reactors agreed well with experimental data.

Introduction

Multiphase catalytic reactors have wide-ranging applications in the chemical industry in a variety of processes in which reactions of gas- and liquid-phase reactants in the presence of solid catalysts are involved. Some important examples are hydroprocessing of petroleum feed stocks, hydrogenation of organic compounds for fine chemicals and pharmaceuticals, oxidation, and hydration (Ramachandran and Chaudhari, 1983; Mills and Chaudhari, 1997). Among the industrial reactors, trickle-bed reactors with down-flow of gas and liquid phases are the most commonly used reactor types, as they are in large-scale processes for hydroprocessing and petrochemicals (Trambouze, 1991). Due to increasing competition and environmental needs, however, alternative modes of operation, such as fixed-bed with upflow of gas and liquid phases, are also gaining considerable attention (Dassori, 1998). The upflow mode may have advantages with respect to uniform liquid distribution, reliable scale-up, selectivity, temperature control and removal of inhibitory byproducts. Therefore, systematic theoretical, and experimental studies on comparison of the reactor performances for downflow (trickle-bed) and upflow modes are most essential.

The analysis of trickle-bed reactors incorporating the contributions of reaction kinetics, external and intraparticle mass transfer, and wetting characteristics of catalyst particles have been extensively studied, including experimental verification of the reactor models (Mills and Dudukovic, 1981; Rajashekharam et al., 1998; Khadilkar et al., 1996, 1998; Bergault et al. 1997). The current state of development on this subject has been reviewed by Al-Dahhan et al. (1997) and Dudukovic et al. (1999). In most cases, the plug-flow models with partial wetting of catalyst particles were found to be representative for trickle-bed reactors at lower liquid velocities. The effect of evaporating solvents (van Gelder et al., 1990a,b), and other

Correspondence concerning this article should be addressed to R. V. Chaudhari.

models based on liquid-flow maldistribution, stagnant liquid pockets in the reactor (Rajashekharam et al., 1998), and mixing cell model (Brahme et al., 1984; Jaganathan et al., 1987) have also been considered. Most of the previous studies on reactor performance have considered single reactions, with a few exceptions wherein complex multistep reactions have been considered under isothermal conditions. An important issue in the design and scale-up of fixed-bed multiphase reactors is the control of temperature, which requires a detailed analysis of nonisothermal effects. In only a few cases has the reactor modeling and experimental verification under nonisothermal conditions been considered in a trickle-bed reactor (Hanika et al., 1977; Rajashekharam et al., 1998; Bergault et al., 1997; Julcour et al., 2000).

The upflow reactor has the advantage of completely wetted catalysts, thus providing better mass transfer and heat transfer between the liquid phase and the solid catalyst. But it has the disadvantage of significant external mass-transfer resistance. Al-Dahhan and Dudukovic (1996) and Wu et al. (1996) have shown that under conditions of liquid-phase reactant limitation, the upflow reactor outperforms the trickle-bed reactor due to its efficient liquid–solid contact. The higher liquid holdup and effective liquid–solid contact also results in a better heat dissipation in the case of exothermic reactions and can be advantageous in reactions where temperature dependence of selectivity is sensitive. Reactor performance studies in upflow reactors for hydrogenation reactions are rare compared to trickle-bed-reactor studies (Mochizuki and Matsui, 1976; Herrmann and Emig, 1998; Stuber et al., 1995), and most of these studies were carried out under isothermal conditions. Nonisothermal reactor performance and theoretical model prediction for upflow reactors are scarce in the literature. Van Gelder et al. (1990a,b) have described a reactor model for the hydrogenation of 2,4,6-trinitrotoluene in an upflow reactor in the presence of an evaporating solvent to absorb the heat of reaction. They have shown that a model incorporating dispersion of the gas phase represents the experimental data better compared to a plug-flow model.

Comparison of the performance for up- and downflow fixed-bed multiphase reactors is necessary to understand clearly the distinguishing features of these two modes. In the previous work, studies on comparison of up- and downflow modes involving both theoretical and experimental aspects have been reported for single reactions under isothermal conditions (DeWind et al., 1988; Goto et al., 1984; Mills et al., 1984;, Leung et al., 1986; Wu et al., 1996; Khadilkar et al., 1996). Some important findings are summarized in Table 1. Comparison of reactor performance under non-isothermal conditions has not been investigated in detail. In a recent report, Julcour et al. (2001) investigated the hydrogenation of 1,5,9-cyclododecatriene (CDT) and observed that the rate of hydrogenation was higher for the upflow mode compared to downflow, in contrast to earlier reports. However, a detailed experimental study on the effect of different parameters under nonisothermal conditions has not been published. The aim of this article is to present a systematic study on the comparison of a fixed-bed reactor in the downflow and upflow modes operated under nonisothermal conditions for the hydrogenation of 1,5,9-CDT using 0.5% palladium on alumina catalyst. Experiments have been carried out over a wide range of operating conditions for both the downflow and upflow modes of operations. For predicting the trickle-bed reactor performance, a nonisothermal plug-flow model taking into consideration the external and intraparticle mass-transfer resistance of a gas-phase reactant (hydrogen) and the wetting characteristics of the catalyst pellets have been developed. For the upflow reactor, the trickle-bed-reactor model has been modified suitably. The effect of liquid flow rate, pressure, and inlet substrate concentration on the performance under the two modes of operation have been studied in the temperature range 373–433 K and model predictions compared with experimental data.

Experimental Studies

Materials

1,5,9-CDT and the catalyst were procured from M/s. Aldrich Chemicals (USA). The catalyst used was 0.5% Pd/Alumina pellets, with an average particle size of 3×10^{-3} m. The solvent used was *n*-decane and was procured from M/s. S.D. Fine Chemicals (India).

Kinetic experiments

For evaluation of intrinsic kinetics, the catalyst pellets were crushed to a fine powder (<50 microns) and the hydrogenation experiments were carried out in a 300-mL capacity autoclave (Parr Instruments, USA), a detailed description of which is given elsewhere (Jaganathan et al., 1999). In a typical experiment, a known amount of catalyst along with 100 mL of CDT solution of known concentration in *n*-decane was charged in the reactor and the contents flushed with nitrogen at room temperature. The heating was then started, and after the desired temperature was reached, the system was pressurized with hydrogen to the desired pressure and the reaction was started by switching the stirrer on. Samples were taken at frequent intervals and analyzed for the reactants and products.

Fixed-bed-reactor experiments

The experiments were carried out in a trickle-bed reactor procured from M/s. "Vinci Technologies," France. The reactor setup is shown in Figure 1. The reactor consists of a stainless steel tube, 0.53 m in length and with a 1.9×10^{-2}m ID. The reactor was also provided with three thermocouples (Chromel–Alumel, type K) to measure temperatures at three different points, namely, along the length of the reactor. A thermo well made of stainless steel with an OD of 0.8×10^{-2} m placed axially along the reactor length had the thermocouples in it. An electronically controlled furnace split into three separate sections heated the reactor, and the corresponding wall temperatures could also be noted from the electronic display along with that of the reactor-bed temperature. The temperature of each of these furnaces could be controlled independently. The gas flow rate was adjusted by a mass-flow controller with a range of 0–60 NL/h and could be read from the electronic display. The reactor pressure was adjusted with the manual pressure controller, and the pressure was indicated by the pressure gauge fitted at the reactor inlet. For quick pressurization of the unit, the mass-flow controller can

Table 1. Experimental Work for Trickle Bed (downflow) and Upflow Modes

Reaction System	Important Observations	Reference
Hydrogenation of α-methylstyrene	(a) In the low interaction regime trickle bed gave higher conversions than upflow	Mills et al. (1984), Wu et al. (1996), Khadilkar et. al. (1996)
	(b) Under conditions of liquid-phase reactant limitation, the upflow reactor is superior. When bed diluted by fines, both reactors perform identically under conditions of both gas-and liquid-phase limitations	
Hydrogenation of diolefin compounds	For better catalyst life and cycle efficiency, upflow reactor is preferable due to effective heat control	Ragaini and Tine (1984)
Oxidation of ethanol	The reaction rates in both reactors were identical in the range studied. However, at lower liquid velocities the rates in trickle-bed reactor are higher	Goto et al. (1984)
Hydration of Isobutene	Reaction rates were higher in upflow reactor	Leung et al. (1986)
Performance of hydro-treating catalysts	Upflow operation gave better utilization of the catalyst	Wind et al. (1988)
Hydrogenation of butadiene	Selectivity better in upflow reactor compared to downflow	Vergel et al. (1993)
Hydrogenation of 1,5,9-cyclododecatriene	Rate of hydrogenation was higher in the upflow mode compared to downflow	Julcour et al. (2000)

be bypassed by a manually operated valve. A storage tank with the liquid feed was kept on a weighing balance with an accuracy of 0.5 g and the exact flow rate of liquid feed was calculated from the weight drop observed from the weighing balance. The pump had a maximum capacity of 2.5×10^{-3} m^3/h. The outlet of the reactor was equipped with a condenser and a high-pressure gas–liquid separator and a liquid-level indicator. The gas outlet line was equipped with a back-pressure controller, which maintained a constant pressure in the unit by continuous pressure release. A wet gas flowmeter measured the total gas outflow. The liquid product from the gas–liquid separator could be drained by means of a

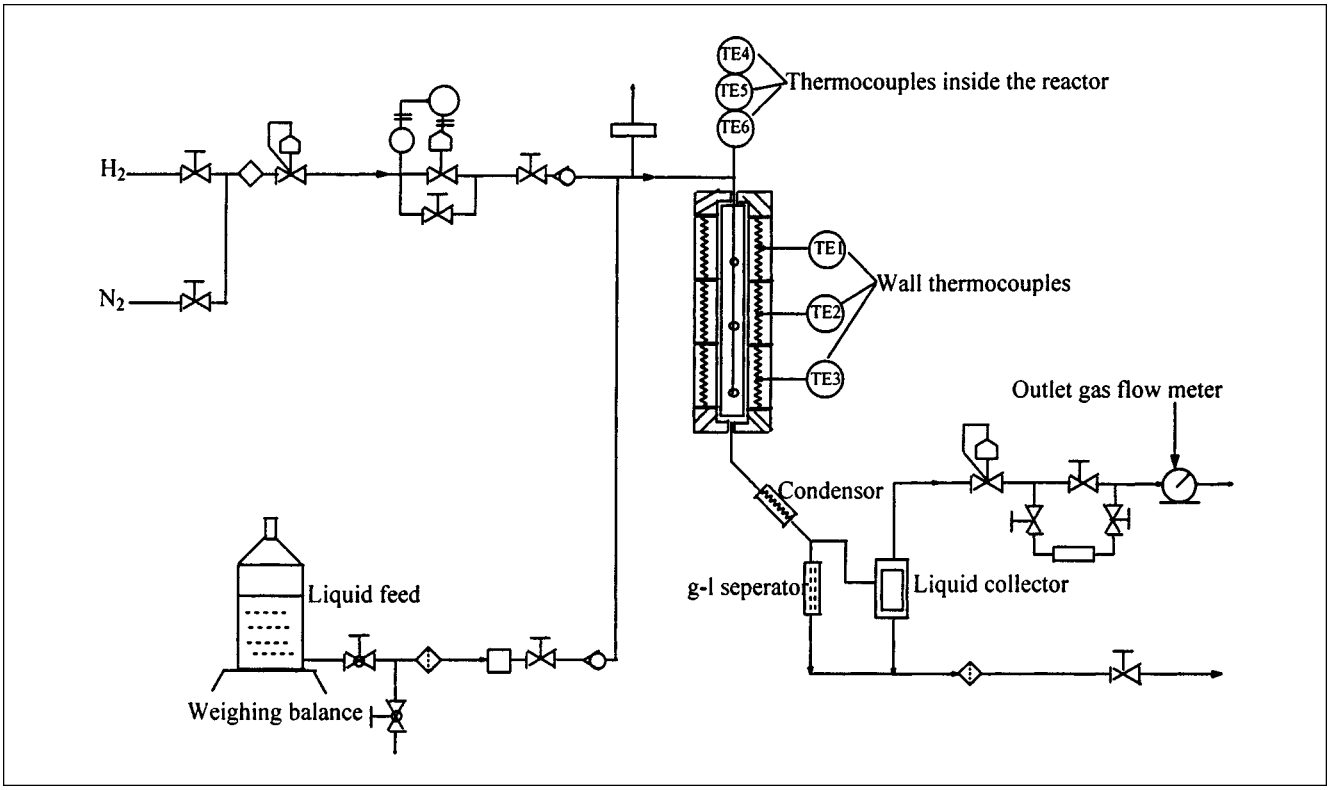

Figure 1. Reactor setup.

"block and bleed valve." In each experiment, the required amount of catalyst was charged in the reactor and the sections above and below the catalyst bed were packed with inert packing (carborundum). The lines of the reactor were flushed with the feed solution before the start of any experiment. In the beginning, the reactor was flushed well with nitrogen and the wall temperatures of the different zones were set to the desired limit. The liquid flow was started after adjusting the required flow rate. Once the temperature of the wall was attained and the temperature inside the reactor was stable, the reactor was pressurized after setting the gas flow rate. Liquid samples were withdrawn from the exit at regular intervals of time and were analyzed by gas chromatography. The temperatures inside the reactor were monitored at three positions inside the reactor. The catalyst was filled in such a way that the first thermocouple was at the inlet of the catalyst bed, the second one was at the middle of the catalyst bed, and the third thermocouple was at the exit of the catalyst bed. Following this procedure, experiments were carried out at different inlet conditions and steady-state performance of the reactor observed by analysis of reactants and products in the exit streams. In all the experiments steady state was reached in about 15 min.

Analysis

Liquid samples were analyzed by gas chromatography (model HP-19091F-102) using a HP-FFAP PEG TPA capillary column of 25 m $\times$ 200 μm $\times$ 0.30 μm. The other conditions of the GC were: injector temperature: 200°C; column temperature: 110 to 140°C programmed at 4°C/min; detector (FID) temperature: 250°C.

Many isomers are formed in the hydrogenation of 1,5,9-CDT. The substrate 1,5,9-CDT used in this work itself contained three isomers: 97% *cis,trans,trans* (ctt), 2% *trans,trans,trans* (ttt), and 0.5 % *cis,cis,cis* (ccc). Stuber et al. (1995) have reported at least 14 different isomers by GC-NMR analysis.

Reactor Model

Intrinsic kinetics

In order to develop rate equations for the different steps in hydrogenation of 1,5,9-CDT using 0.5% Pd/alumina catalyst, experiments were carried out in a batch slurry reactor using the powdered catalyst and *n*-decane as a solvent. Though the kinetics of this reaction has been investigated before (Benaissa et al., 1996; Stuber et al., 1995) using pure CDT as the feedstock and 0.5 % Pd/alumina (supplied by Degussa, Germany), it was thought necessary to determine the kinetic parameters for the specific catalyst (0.5% Pd/alumina supplied by Aldrich, USA) and solvent (*n*-decane) used in this study. A number of isomers of intermediate products are formed during the hydrogenation, but the main products are cyclododecadiene (CDD), cyclododecene (CDE), and cyclododecane (CDA). The different isomers observed include four CDT, three CDD, and two CDE isomers. Furthermore, two CDT and three CDD positional isomers were also found, though the concentration of these positional isomers was negligible.

In this work, a lumped reaction scheme as shown below was considered for kinetic modeling

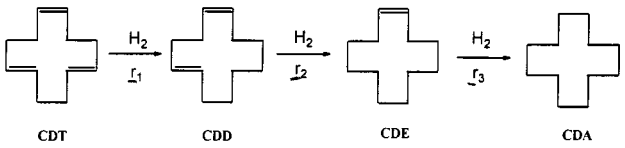

Experiments were carried at different catalyst loadings, hydrogen partial pressures, and initial CDT concentrations in a temperature range from 353 K to 398 K, in which concentration-time data were obtained. The procedure followed for kinetic modeling was similar to that discussed earlier (Benaissa et al., 1996). Langmuir-Hinshelwood type of rate equations given below were found to represent the data satisfactorily, as evidenced by the comparison between the experimental and predicted results shown in Figure 2 for 353 and 373 K.

$$r_1 = \frac{wk_1 BA^*}{(1 + K_B B + K_c C + K_E E)} \tag{1}$$

$$r_2 = \frac{wk_2 CA^*}{(1 + K_B B + K_c C + K_E E)} \tag{2}$$

$$r_3 = \frac{wk_3 EA^*}{(1 + K_B B + K_c C + K_E E)}, \tag{3}$$

where A^* represents the dissolved hydrogen concentration in equilibrium with the gas phase, kmol/m^3, and B, C, and E represent concentrations of CDT, CDD, and CDE, respectively in kmol/m^3. The rate parameters evaluated for Eqs. 1 to 3 are presented in Table 2. The activation energies for the rate constants k_1, k_2, and k_3 were found to be 41, 41 and 35 kJ/mol, respectively. The activation energies for the constants K_B, K_C, and K_E were 14.8, 15.21 and 15.0 kJ/mol, respectively.

The activation energies are somewhat low, which may indicate transport limitations. However, we have ensured by well-known criteria involving the comparison of the rate of hydrogenation with the maximum rate of gas–liquid, liquid–solid, and intraparticle diffusion rates, that mass-transfer resistances were unimportant under the conditions of kinetic study (Jaganathan et al., 1999; Rajashekharam et al., 1997).

Trickle-bed reactor model

A trickle-bed-reactor model for hydrogenation of CDT was developed similar to that proposed earlier (Rajashekharam et al., 1998). The salient features of the model are: the spherical catalyst particle was assumed to be divided into three zones that represented (1) a dry zone, (2) a wetted zone covered by the flowing dynamic liquid and (3) a wetted zone covered by the stagnant liquid. It was assumed that (a) gas and liquid phases are in plug flow; (b) the liquid-phase reactant is nonvolatile and is in excess compared to the gaseous reactant

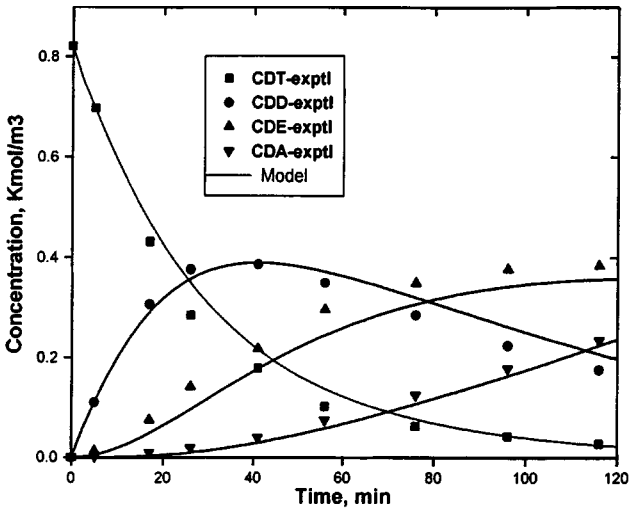

Figure 2. Concentration-time profiles in a batch slurry reactor (a) 353 K; (b) 373 K.

Reaction conditions: initial concentration of CDT: 0.82 kmol/m^3; pressure: 1.2 MPa; catalyst loading: 1.82 kg/m^3; agitation speed: 1,100 rpm.

concentration in the liquid phase; (c) the gas–liquid, liquid–solid, and intraparticle mass-transfer resistances for H_2 are considered, whereas the liquid–solid and intraparticle mass-transfer resistances for the liquid-phase components are assumed to be negligible; (d) the interphase and intraparticle heat-transfer resistances are negligible, but bed-to-wall heat transfer has been considered to incorporate the non-isothermal effects; (e) the overall catalytic effectiveness factor can be expressed as a sum of the weighted average of the effectiveness factors in the dynamic liquid-covered, stagnant-liquid-covered, and gas-covered zones, respectively, that is,

$$\eta = f_d\eta_d + f_s\eta_s + (1 - f_d - f_s)\eta_g, \tag{4}$$

where η is the overall catalytic effectiveness factor under conditions of partial wetting and stagnant liquid pockets, and f_d and f_s are the fractions of catalyst particle covered by the dynamic and stagnant-liquid zones; and η_d, η_s, and η_g are the overall effectiveness factors for dynamic, stagnant, and dry zones, respectively. For conditions of complete wetting and absence of stagnant-liquid pockets $\eta = \eta_c$.

The catalytic effectiveness factor equations applicable to hydrogenation of CDT were developed following the well-known approaches (Bischoff, 1965; Ramachandran and Chaudhari, 1983). Under the conditions of significant intraparticle gradients for the gas-phase reactant (H_2) and when the liquid-phase reactant is in excess, the overall rate of hydrogenation can be expressed as (combining Eqs. 1–3)

$$R_A = \frac{\eta w(k_1B_1 + k_2C_1 + k_3E_1)A^*}{(1 + K_BB_1 + K_cC_1 + K_EE_1)}, \tag{5}$$

where η is given by Eq. 4 and η_c is given by the following expression for a spherical catalyst particle:

$$\eta_c = \frac{1}{\phi}\left(\coth 3\phi - \frac{1}{3\phi}\right), \tag{6}$$

where ϕ is the Thiele parameter defined as

$$\phi = \frac{R}{3}\left[\frac{S_p(k_1B_1 + k_2C_1 + k_3E_1)}{D_e(1 + K_BB_1 + K_EC_1 + K_EE_1)}\right]^{1/2}, \tag{7}$$

or in dimensionless form as

$$\phi = \phi_0\left[\frac{(b_1 + k_{21}c_1 + k_{31}e_1)}{(1 + k_bb_1 + k_cc_1 + k_ee_1)}\right]^{1/2} \tag{8}$$

Table 2. Kinetic Parameters

Temp. (K)	$k_1 \times 10^2$ (m^3/kg) m^3/kmol/s)	$k_2 \times 10^2$ (m^3/kg) m^3/kmol/s)	$k_3 \times 10^2$ (m^3/kg) (m^3/kmol/s)	K_B (m^3/kmol)	K_C (m^3/kmol)	K_D (m^3/kmol)
333	1.480	0.488	0.384	5.101	2.472	2.399
353	3.465	1.123	0.899	2.198	1.049	0.978
373	7.415	2.401	1.921	1.021	0.440	0.482
393	14.61	4.750	3.809	0.521	0.252	0.209

$$\phi_0 = \frac{R}{3}\left[\frac{\rho_p k_1 B_{1_i}}{D_e}\right]^{1/2}. \quad (9)$$

The dimensionless mass-balance equations for the different species involved in the reaction are given below. [The detailed derivation is taken from our earlier article, (Rajashekharam et al., 1998)]. The dimensionless mass-balance equation for species A (hydrogen) is

$$\frac{da_{1_d}}{dz} + \alpha_{gl}\left(1 - a_{1_d}\right) = \frac{\eta_c \alpha_r (b_1 + k_{21}c_1 + k_{31}e_1)}{(1 + k_b b_1 + k_c c_1 + k_e e_1)} \times \left\{ \frac{f_d a_{1_d}}{\left(1 + \eta_c \phi^2/N_d\right)} + \frac{f_s a_{1_d}}{\left(1 + \eta_c \phi^2/N_s\right) + \left(\eta_c \phi^2/\alpha_s N_s\right)} \right\}, \quad (10)$$

with

$$(1 - f_d - f_s)\alpha_{gs}\left(1 - a_{s_g}\right) = (1 - f_d - f_s) \times \frac{\eta_c \alpha_r (b_1 + k_{21}c_1 + k_{31}e_1)}{(1 + k_b b_1 + k_c c_1 + k_e e_1)} \times \left[\frac{1}{\left(1 + \eta_c \phi^2/N_g\right)}\right]. \quad (11)$$

The mass balances of liquid-phase reactants/products in dimensionless form are given as

$$-\frac{db_{l_d}}{dz} = \frac{\eta_c \alpha_r b_1 \chi}{q_B\left(1 + k_b b_l + k_c c + k_e e_{l_l}\right)} \quad (12)$$

$$\frac{dc_{l_d}}{dz} = \frac{\eta_c \alpha_r (b_l - k_{31}c_l)\chi}{q_B(1 + k_b b_l + k_c c_l k_e e_l)} \quad (13)$$

$$\frac{de_{l_d}}{dz} = \frac{\eta_c \alpha_r (k_{21}c_l - k_{41}e_l)\chi}{q_B(1 + k_b b_l + k_c c_l k_e e_l)} \quad (14)$$

$$\frac{dp_{l_d}}{dz} = \frac{\eta_c \alpha_r k_{31} e_1 \chi}{q_B(1 + k_b b_l + k_c c_l + k_e e_l)}, \quad (15)$$

with

$$\chi = \left\{ \frac{f_d a_{l_d}}{\left(1 + \eta_c \phi^2/N_d\right)} + \frac{f_s a_{l_d}}{\left[\left(1 + \eta_c \phi^2/N_s\right) + \left(\eta_c \phi^2/\alpha_s N_s\right)\right]} + \frac{(1 - f_d - f_s)}{\left(1 + \eta_c \phi^2/N_g\right)} \right\}. \quad (16)$$

The dimensionless parameters used in the preceding equations are defined in Table 3. In deriving a nonisothermal trickle-bed-reactor model, the dependencies of various parameters like reaction rate constants, equilibrium constants, effective diffusivity, and saturation solubility on temperature are accounted for. The effective diffusivity was calculated as

$$D_e(T_o) = D_m \frac{\epsilon}{\tau}, \quad (17)$$

where D_m is the molecular diffusivity and is evaluated from the correlation of Wilke and Chang (1955), and ϵ and τ represent the porosity and the tortuosity factors. The porosity and tortuosity values were taken as 0.45 and 7.2, respectively (Stuber et al., 1995). The variation of the vapor pressure with temperature for the solvent *n*-decane was calculated from the following equations reported in the literature (Stephan and Stephan, 1963)

$$\log(P_v)_T = \frac{0.2185 \times 10{,}912}{T} + 8.24889. \quad (18)$$

Table 3. Dimensionless Parameters Used in the Model

Mass transfer parameters	
Gas–liquid mass transfer	$\alpha_{g=} k_l a_B L/U_l$
Liquid–solid mass transfer	$\alpha_{ls} = k_s a_p L/U_l$
Gas–solid mass transfer	$\alpha_{gs} = k_{gs} a_p L/U_l$
Nusselt number in dynamic zone	$N_d = Rk_{s_d}/3D_e$
Nusselt number in stagnant zone	$N_s = Rk_{s_g}/3D_e$
Nusselt number in dry zone	$N_g = Rk_{g_s}/3D_e$
Thiele parameter	$\phi = R/3(\rho_p k_l B_{l_i}/D_e)^{0.5}\left[\frac{b_l + k_{21}c_l + k_{31}e_l}{1 + k_b b_l + k_c c_l + k_e e_l}\right]^{0.5}$
Exchange parameter for stagnant zone	$\alpha_s = (k_{ex}\epsilon_l/f_s k_{s_s} a_p)$
Heat-transfer parameter	
Thermicity parameter	$\beta_1 = \frac{(-\Delta H)B_{l_i}}{T_o C_{p_i}\rho_l(1 + [U_g C_{p_g}\rho_g/U_l C_{p_l}\rho_l])}$
Bed-to-wall heat transfer	$\beta_2 = \frac{4U_w L}{d_T C_{p_l}\rho_l(1 + [U_g C_{p_g}\rho_g/U_l C_{p_l}\rho_l])}$
Reaction rate and equilibrium constants	$\alpha_r = Lwk_l B_{l_i}/U_l$ $k_{21} = k_2/k_1;\ k_{31} = k_3/k_{11}$ $k_b = K_B B_{l_i}\ k_c = K_C B_{l_i}$

Since dilute solutions of CDT were used in the present study, the vapor pressure of CDT was neglected in the calculations. The solubility of hydrogen in the CDT–*n*-decane mixture was determined experimentally, and the Henry's constant of solubility, H_e, was expressed by the following correlation

$$(H_e)_T = -1.9\times10^{-3} + 1.82\times10^{-5}T - 1.89\times10^{-5}Y, \quad (19)$$

where T is the temperature, Y is the concentration of CDT in % (w/w), and $(H_e)_T$ is the Henry's constant expressed as kmol/m^3/atm.

The heat evolved during the reaction was assumed to be carried away by the flowing liquid and transfer to the reactor wall, which is characterized by the bed-to-wall heat-transfer coefficient, U_w. Under such conditions, where the interphase and intraparticle heat-transfer resistances are assumed to be negligible, the heat balance of the reactor can be expressed in dimensionless form as (Ramachandran and Chaudhari, 1983)

$$\frac{d\theta}{dz} = \frac{\eta_c \alpha_r \beta_1 (b_l + k_{21}c_l + k_{31}d_l)\chi}{q_B(1k_B b_L + k_C c_L + k_E e_L)} - \beta_2(\theta_b - \theta_W), \quad (20)$$

where β_2 is the thermicity parameter and other dimensionless parameters are given in Table 3. Equations 10 to 15 combined with Eq. 20 were solved using a fourth-order Runge-Kutta method to predict the concentrations of reactants/products and the temperature along the length of the reactor with the following initial conditions:

$$\text{at} \quad z = 0; \qquad a_1 = b_1 = 1; \qquad c_1 = e_1 = p_1 = 0; \quad (21)$$

From these results, the conversion of CDT (X_B) was calculated as

$$X_B = 1 - b_1. \quad (22)$$

The global rate of hydrogenation (including hydrogen consumption in all the steps) was calculated as:

$$R_A = \frac{U_1}{L}(C_1 + 2E_1 + 3P_1), \quad (23)$$

where U_l is the liquid velocity in m/s, L is the length of the catalyst bed in m, C_l, E_l, P_l are the concentrations of CDD, CDE, and CDA, respectively, at the exit of the reactor,

Table 4. Correlations Used for Downflow Modeling

Parameter	Correlation	Reference
Gas–liquid mass-transfer coefficient	$\frac{K_L a_B d_p}{D(l-\epsilon_L/\epsilon_B)} = 2\left(\frac{S_p}{d_p^2}\right)^{0.2} Re_L^{0.73} Re_G^{0.2} \left(\frac{\mu_L}{\rho_L D}\right)^{0.5} \left(\frac{d_p}{d_T}\right)^{0.2}$	Fukushima and Kusaka (1977)
Liquid–Solid mass-transfer coefficient	$\frac{K_s d_p}{D}\frac{a_w}{a_p} = 0.815\mathrm{Re}_\mathrm{L}^{0.822}\left(\frac{\mu_l}{\rho_L D}\right)^{0.333}$	Satterfield et al. (1978)
Volumetric mass-exchange coefficient	$K_{ex} = 0.01 Re_L^{0.6}$	Hochmann and Effron (1969)
Total liquid holdup	$\frac{\epsilon_L}{\epsilon_B} = 0.185 a_\mathrm{t}^{1/3}\chi^{0.22}$	Sato et al. (1973)
Bed-to-wall heat-transfer coefficient	$\frac{h_w d_p}{\lambda_L} = 0.057\left(\frac{Re_L}{\epsilon_L}\right)^{0.09} Pr_L^{1/3}$	Baldi (1981)
Wetting efficiency	$\eta_{CE} = 1.104 Re_L^{1/3}\left[\frac{1+[(\Delta P/Z)/\rho_L g]}{Ga_L}\right]^{1/9}$	Al-Dahan et al. (1997)

Table 5. Correlations Used for Upflow Modeling

Parameter	Correlation	Reference
Gas–liquid mass-transfer coefficient, $k_L a_B$	$k_L a_B = 5.48\times10^{-3}\,[U_l \delta_{gl}]^{0.5}$	Reiss (1967)
Pressure drop per unit length of reactor, δ_{gl}	$[\delta_{gl}]^{0.5} = \frac{2 f_{gl} U_g^2 \rho_g}{d_{pe}}$	Turpin and Huntington (1967)
Liquid–solid mass-transfer coefficient, k_s	$k_s = \left(0.48\ln\left(\frac{Re_G 10^2}{Re_L}\right) - 0.03\left(\ln\left(\frac{Re_G 10^2}{Re_L}\right)\right)^2 - 0.3\right)\frac{D_{12} Sh_0}{d_p}$	Specchia et al. (1978)
Liquid holdup, ϵ_l	$\epsilon_1 = \epsilon_B 1.47 Re_l^{0.11} Re_G^{-0.19} (a_p d_p)^{-0.41}$	Stiegel and Shah (1977)

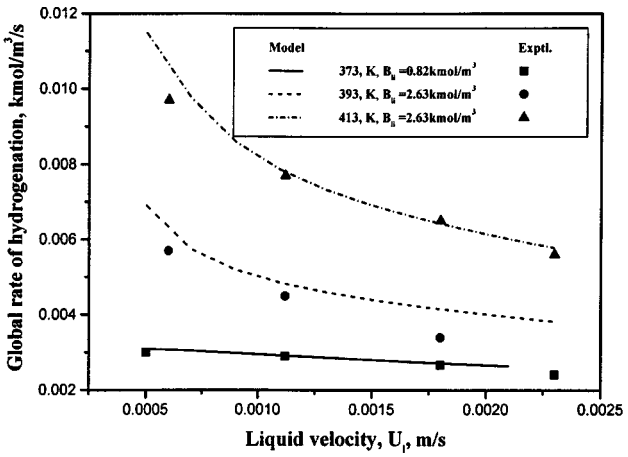

Figure 3. Effect of liquid velocity on global hydrogenation rate in trickle bed (downflow) at different inlet temperatures.

Reaction conditions: $P_H = 1.2$ MPa; $U_g = 3.9 \times 10^{-3}$ m/s.

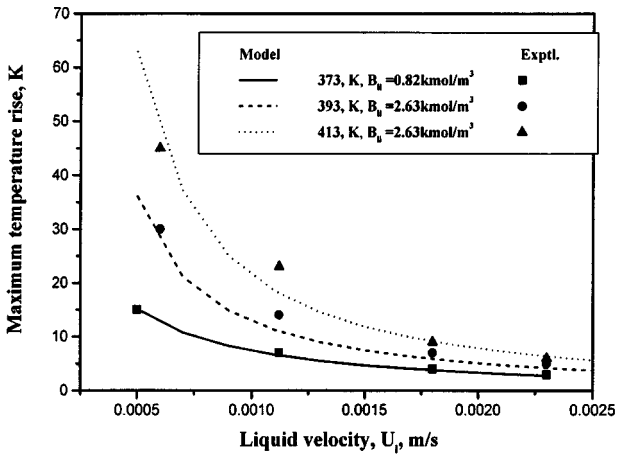

Figure 5. Effect of liquid velocity on maximum temperature rise (ΔT) in trickle bed (downflow) at different inlet temperatures.

Reaction conditions: inlet CDT = 0.82 kmol/m^3; $P_H = 1.2$ MPa; $U_g = 3.9 \times 10^{-3}$ m/s.

kmol/m^3. The model parameters were evaluated using correlations given in Table 4.

Model for upflow reactor

The model equations described earlier for the downflow reactor can also be used for the upflow reactor with appropriate modifications and relevant parameters. Since the catalyst is completely wetted in the upflow operation, the wetting efficiency was taken as unity. The correlations used for evaluation of hydrodynamics and mass-transfer parameters for the upflow mode are presented in Table 5.

For the simulation of experimental data with model predictions, we have used literature correlations except for the bed-to-wall heat-transfer coefficient, for which reliable correlations are not available. The strategy followed was to fit this parameter (bed-to-wall heat-transfer coefficient) using one or two sets of experimental data at different gas and liquid velocities. These parameters were then used at appropriate gas and liquid velocities for simulation of results under a wide range of conditions.

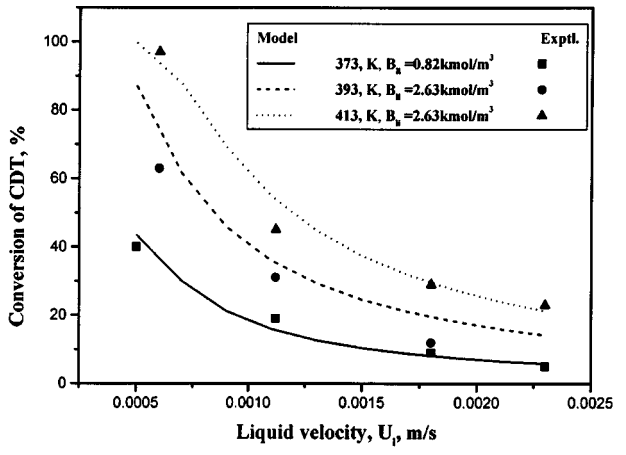

Figure 4. Effect of liquid velocity on conversion of CDT in trickle bed (downflow) at different inlet temperatures.

Reaction conditions: $P_H = 1.2$ MPa; $U_g = 3.9 \times 10^{-3}$ m/s; $U8Dg = 3.9 \times 10^{-3}$ m/s.

Results and Discussion

Experimental data were obtained for both trickle-bed (downflow) and upflow modes of operation, in which liquid velocity, pressure of hydrogen, inlet concentration of CDT, and temperature were varied. In the following sections, the effect of these parameters on the overall rate of hydrogenation, conversion of CDT, and temperature rise is discussed. The results have been compared with model predictions for each mode of operation, and the reactor performance for the two modes is also compared based on experimental data obtained under identical conditions.

Trickle-bed-reactor performance

Effect of Liquid Velocity. The effect of liquid velocity on the global rate of hydrogenation, temperature rise, and CDT conversion is shown in Figures 3–5. The global rate of hydrogenation and CDT conversion was found to decrease with an increase in liquid velocity. Similarly, the temperature rise decreased with an increase in liquid velocity at all the inlet temperatures studied (Figure 5). With increase in liquid velocity, one expects increase in wetted fraction of the catalyst as well as an increase in the gas-liquid and liquid-solid mass-transfer coefficients. At lower liquid velocity, catalyst particles are partially wetted, and under these conditions, it is well known that the rate increases due to direct transfer of the gas-phase reactant to the catalyst surface (already wetted internally due to capillary forces). Hence, with an increase in liquid velocity, an increase in the wetted fraction is expected to retard the rate of reaction, while an increase in the external mass-transfer coefficients will enhance the rate, resulting in opposite

effects. Superimposed on these effects would be the effect of an increase in bed temperature due to exothermicity. At 373 K, wherein the temperature rise over the entire varied liquid-velocity range is less than 10 K, the liquid-velocity effect is not very significant, perhaps due to the compensation of the effect of wetting and the increase in external mass-transfer coefficients. But at a higher inlet temperature, 413 K, the rate decreases sharply with liquid velocity due to the large difference in the temperature rise. With the increase in liquid velocity, the heat evolved due to exothermicity is removed at a significantly higher rate, resulting in a reduced bed temperature rise and rate of reaction. For example, at $U_l = 5\times10^{-4}$ m/s, ΔT was observed as 45 K, while at $U_l = 2.1\times10^{-3}$ m/s, ΔT was 6 K. Thus, the trickle-bed-reactor performance under nonisothermal conditions is significantly different from that under isothermal conditions.

In order to compare the experimental data with model predictions, Eqs. 10 to 15 and 20, with the initial condition in Eq. 21, were solved numerically to obtain exit concentrations of all the reactants, intermediates, and products, as well as the temperature along the axis for the conditions used in the experiments. From these data, the conversion of CDT (X_B), the global rate of hydrogenation (R_A), and the temperature rise (ΔT) along the length of the reactor for a given set of input conditions were calculated. Besides the kinetic parameters (Table 2), other key parameters in the model for nonisothermal trickle-bed reactor (downflow operation) are wetted fraction of the catalyst particles, gas–liquid mass transfer, gas–particle mass-transfer (to the unwetted portion of the catalyst) coefficient, liquid–solid mass-transfer coefficients for the dynamic and stagnant-liquid-covered zones, effective diffusivity, and overall heat-transfer coefficient. For comparison of the experiments with model predictions, temperature rise was calculated based on the temperature at $z = 0.5$, where the temperature in the bed could be measured. A comparison of the model predictions with experimental data is also shown in Figures 3–5 for 373, 393, 413 K, which shows excellent agreement.

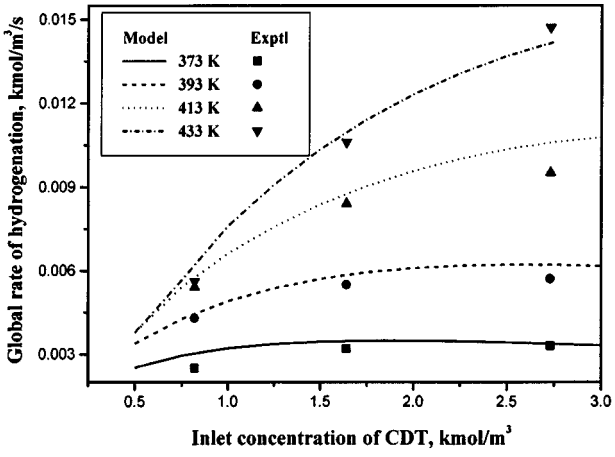

Figure 6. Effect of inlet CDT concentration on global rate of hydrogenation in trickle-bed reactor (downflow).

Reaction conditions: $P_H = 1.2$ MPa; $U_l = 1.2\times10^{-3}$ m/s; $U_g = 3.9\times10^{-3}$ m/s.

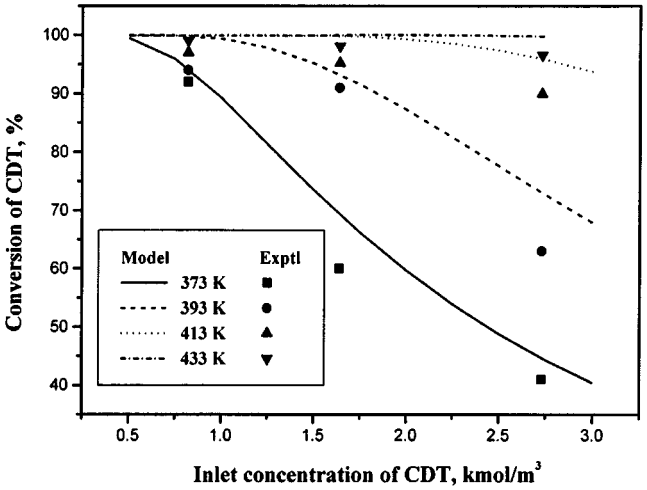

Figure 7. Effect of inlet CDT concentration on conversion of CDT in trickle-bed reactor (downflow).

Reaction conditions: $P_H = 1.2$ MPa; $U_l = 1.2\times10^{-3}$ m/s; $U_g = 3.9\times10^{-3}$ m/s.

Effect of Inlet CDT Concentration. The effect of CDT concentration in the inlet on global rate of hydrogenation, conversion of CDT, and maximum temperature rise is shown in Figures 6–8 for different temperatures. The conversion of CDT was found to decrease with the increase in CDT concentration, as expected, while the global rate of hydrogenation and temperature rise were found to increase with CDT concentration. The effect of CDT concentration on the rate and ΔT was found to be significant at higher inlet temperatures. At a higher inlet feed temperature (413 K), a temperature rise as high as 65 K was observed, while at a lower inlet temperature (373 K), it was only about 10 K. A comparison of these experimental data with model predictions (Figures 6–8) shows good agreement.

Effect of Hydrogen Pressure. The effect of hydrogen pressure on the global rate of hydrogenation and ΔT is shown in Figure 9 along with model predictions. Here again a good agreement between the experiments and the model prediction was observed, indicating the applicability of the model over a wide range of conditions. As expected, the rate as well as the temperature rise were found to increase with an increase in pressure. At higher operating pressures the temperature rise in the catalyst bed and the global rate of hydrogenation increased nearly in a linear manner (Figure 9).

Comparison of trickle bed with upflow mode

Experiments were also carried out on hydrogenation of CDT in a fixed-bed reactor with upflow of liquid and gas at different liquid velocities, inlet temperatures, CDT concentrations, and hydrogen pressures. The results, along with comparison of the data for trickle bed (downflow) under identical conditions, are discussed below.

Effect of liquid velocity. The effect of liquid velocity on the global rate of hydrogenation was marginal for both upflow and downflow operations at 373 K inlet temperature, though the rate was significantly higher in a trickle-bed reactor at 413 K (Figure 10). In a trickle-bed reactor, the rate

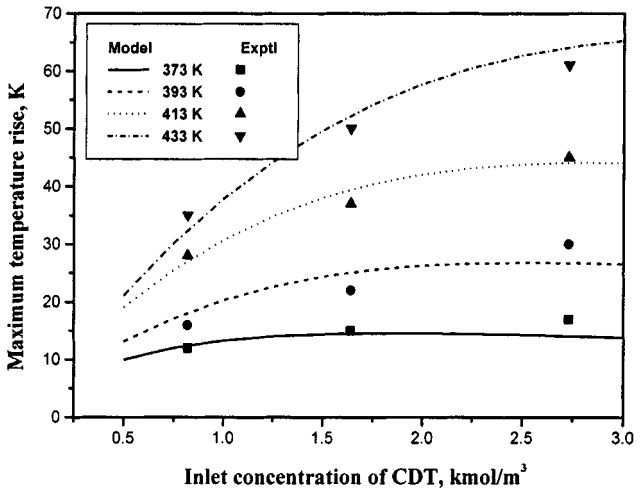

Figure 8. Effect of inlet CDT concentration on maximum temperature rise (ΔT) in a trickle-bed reactor (downflow).

Reaction conditions: $P_H = 1.2$ MPa; $U_l = 1.2 \times 10^{-3}$ m/s; $U_g = 3.9 \times 10^{-3}$ m/s.

decreased by 20%, but in the upflow mode, it increased by only 6% with a 4-fold increase in U_l. In the upflow mode, catalyst particles are completely covered by liquid, whereas in the trickle bed, a significant partial wetting exists in the varied range of U_l. The higher rate for the trickle bed is due to the direct mass transfer of gas-phase reactant to the catalyst surface, eliminating gas–liquid and liquid–solid mass-transfer resistance. Since the rate of the gas-particle mass-transfer rate is generally higher than the other steps, a significant rate enhancement is expected. In the previous work, Julcour et al. (2000) observed that the rate was higher for the upflow mode compared to trickle bed for the same reaction system in contrast to the observations made here. However, these two studies have led to different results mainly because, in the previous work a diluted catalyst bed (100 g of catalyst mixed with 500 g of inert) was used in a pilot-scale reactor of about one-liter capacity, while for the present work an undiluted catalyst bed was used in a smaller bench-scale reactor of 100-cm^3 capacity. Indeed, the present work allowed us to consider the analysis of some differences due to scale-up operation and the dilution of the catalyst bed. The most significant effect of the dilution of the catalyst bed is on the wetting efficiency and misdistribution of liquid flowing in the trickle-bed reactor, and the different trends observed in the results in these two studies is a result of the differences in the hydrodynamic conditions due to bed dilution. The effect of the liquid velocity on the conversion of CDT and rise in temperature are shown in Figures 11 and 12. In the trickle-bed reactor, higher conversion and a higher rise in temperature was observed, but for the upflow mode, the rise in temperature was much lower due to efficient heat removal.

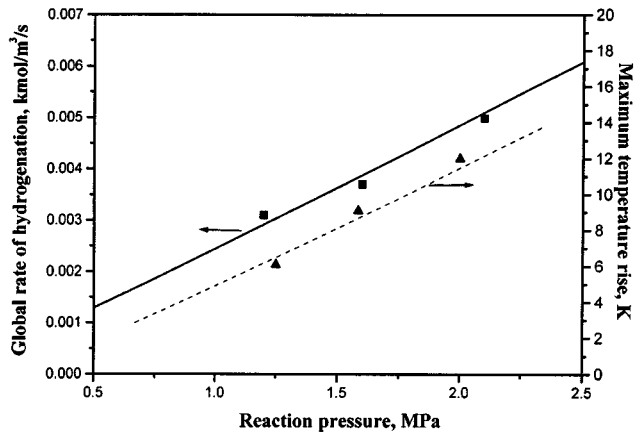

Figure 9. Effect of hydrogen pressure on global rate and temperature in a trickle bed (downflow)

Reaction conditions: T : 373 K, Inlet CDT = 0.82 kmol/m^3; $U_l = 1.2\text{x}10^{-3}$ m/s; $U_g = 3.9 \times 10^{-3}$ m/s.

Effect of Pressure, Temperature, and Inlet CDT Concentration. The effect of hydrogen pressure and inlet temperature on the reactor performance is shown in Figures 13 and 14

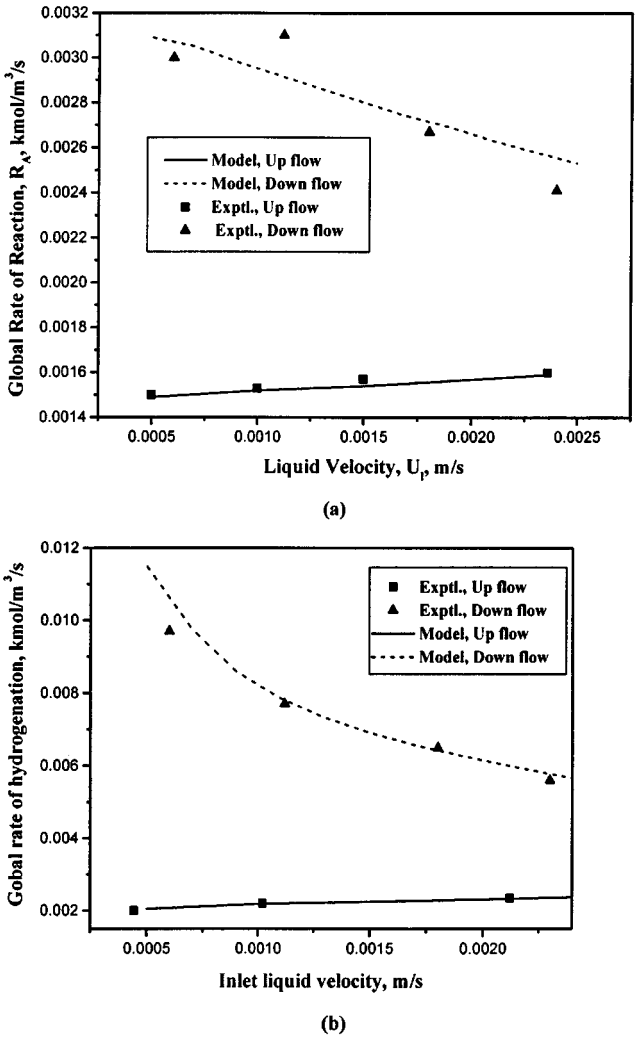

Figure 10. Effect of liquid velocity on global rate of hydrogenation in trickle-bed and up-flow modes.

Reaction conditions: $P_H = 1.2$ MPa; $U_g = 3.9 \times 10^{-3}$ m/s. (a) $T = 373$ K; inlet CDT = 0.82 kmol/m^3; (b) $T = 413$ K, inlet CDT = 2.63 kmol/m^3.

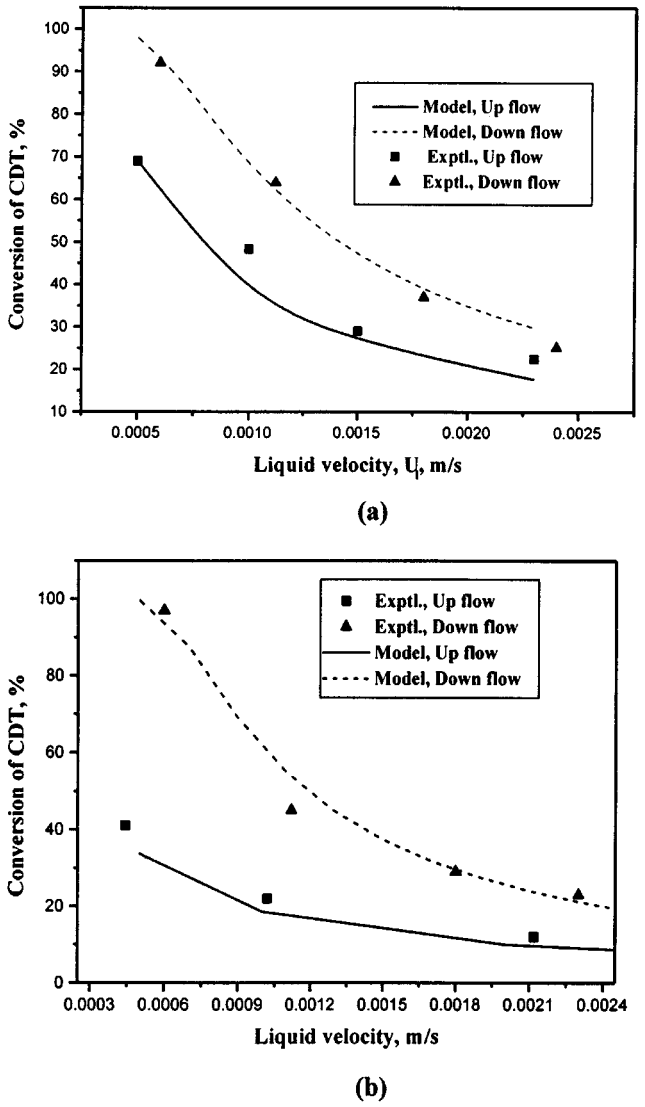

Figure 11. Effect of liquid velocity on conversion of CDT in trickle-bed and upflow modes.

Reaction conditions: $P_H = 1.2$ MPa; $U_g = 3.9 \times 10^{-3}$ m/s, (a) $T = 373$ K; inlet CDT = 0.82 kmol/m^3; (b) $T = 413$ K, inlet CDT = 2.63 kmol/m^3.

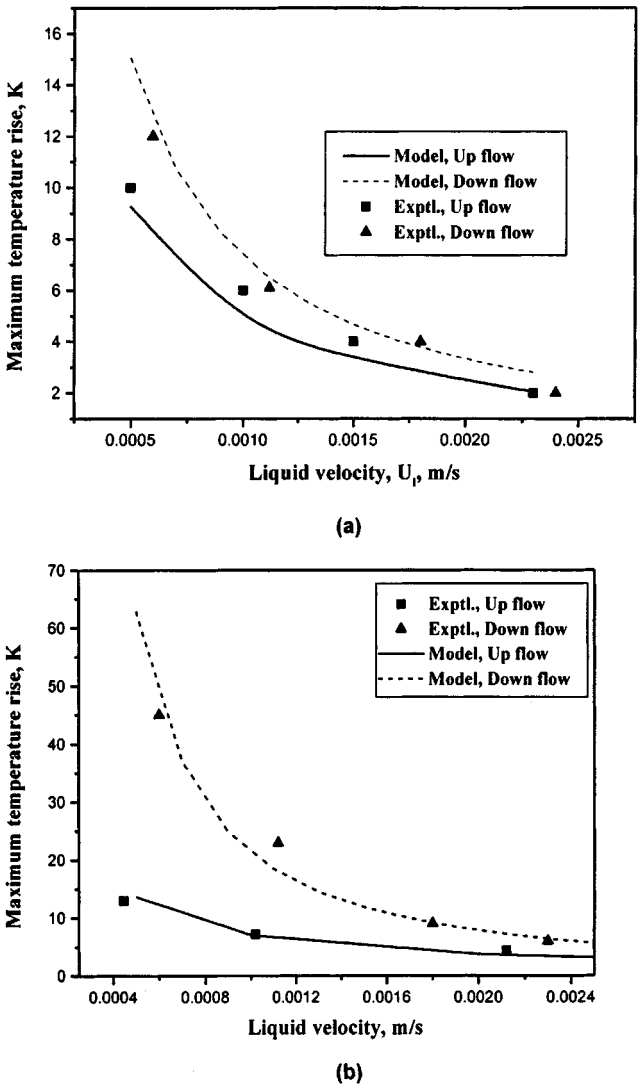

Figure 12. Effect of liquid velocity on temperature rise in trickle-bed and upflow modes.

Reaction conditions: $P_H = 1.2$ MPa; $U_g = 3.9 \times 10^{-3}$ m/s. (a) $T = 373$ K; inlet CDT = 0.82 kmol/m^3; (b) $T = 413$ K, inlet CDT = 2.63 kmol/m^3.

and Figures 15 and 16, respectively, for the downflow and upflow modes. The effect of inlet CDT concentration is shown in Figures 17 and 18. In all cases, the global reaction rate and temperature rise were higher for the downflow compared to upflow. This difference is mainly due to the partial wetting of catalyst particles in the downflow mode, which is known to enhance the overall rate, as discussed earlier. The observation of a lower rise in temperature in the upflow mode is due to more efficient heat removal, which can be advantageous in temperature control for exothermic reactions. The experimental data over a wide range of conditions were found to agree well with model predictions for both the modes.

Selectivity behavior

A comparison of the selectivity of CDE in the two reactor modes is shown in Figures 19 to 22 for different liquid velocities, hydrogen pressure, inlet CDT concentration, and inlet temperature. In general, the selectivity of CDE compared to other products (CDD and CDA) was found to be higher in the trickle-bed reactor for all conditions. The selectivity of CDE is expected to be proportional to the global rate of hydrogenation rather than CDT conversion, and since in most conditions the global rate was higher in the trickle bed, the CDE selectivity was also higher. In the previous work (Julcour et al., 2000), the global rate was higher for the upflow operation compared to trickle bed and the selectivity of CDE defined as the ratio of [(CDE/(CDE + CDA)) × 100] was also higher for the upflow mode. For the present work, the selectivity defined as [(CDE/(CDE + CDA)) × 100] was higher for upflow, as was that observed by Julcour et al. (2000); however, the selectivity in relation to all the products [(CDE/(CDD + CDE + CDA)) x100] was found to be higher

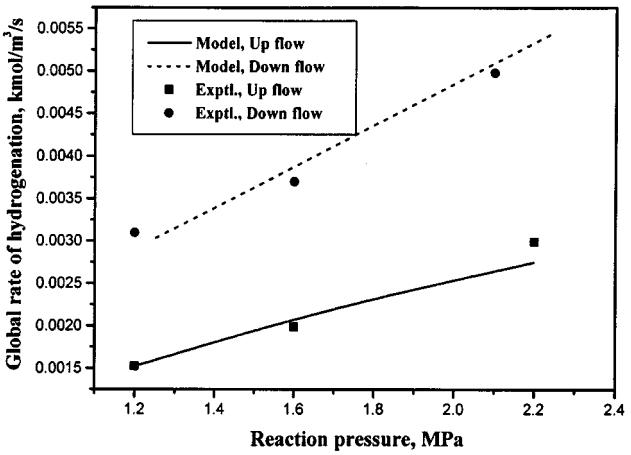

Figure 13. Effect of hydrogen pressure on global rate of hydrogenation in trickle-bed and upflow modes.

Reaction conditions: T = 373 K, inlet CDT = 0.82, kmol/m^3; $U_l = 1.2\times10^{-3}$; m/s; $U_g = 3.9\times10^{-3}$ m/s.

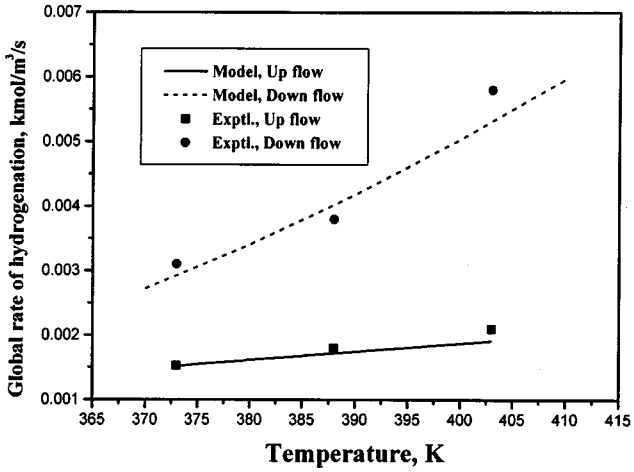

Figure 15. Effect of inlet temperature on global rate of hydrogenation in trickle-bed and upflow modes.

Reaction conditions: inlet CDT = 0.82 kmol/m^3; P_H = 1.2 MPa; $U_l = 1.2\times10^{-3}$ m/s; $U_g = 3.9\times10^{-3}$ m/s.

in the downflow mode. This is due to significant formation of CDA in the trickle compared to the upflow mode.

Conclusions

The hydrogenation of 1,5,9-CDT using 0.5% palladium on alumina as the catalyst was investigated under nonisothermal conditions in a trickle-bed (downflow) as well as the upflow mode. The effect of liquid velocity, hydrogen pressure, and inlet CDT concentration on the global rate of hydrogenation, CDT conversion, temperature rise, and CDE selectivity was studied in a temperature (inlet) range of 373–413 K. Theoretical models for the trickle-bed and upflow modes have been developed that incorporate the contributions of external and intraparticle mass transfer, partial wetting of catalyst (for downflow), overall heat transfer, and complex reaction kinetics applicable to hydrogenation of CDT. The experimental data over a wide range of conditions were found to agree well with model predictions for both the modes.

The comparison of the reactor performance in the two modes indicated that (1) trickle bed (downflow) gives a higher rate of reaction as a result of partial wetting phenomena. Comparison of the results with previous work indicated that for diluted catalyst beds, the performance of the upflow mode is higher than trickle bed due to poor utilization of catalyst in the downflow mode as a result of channeling of liquid flow

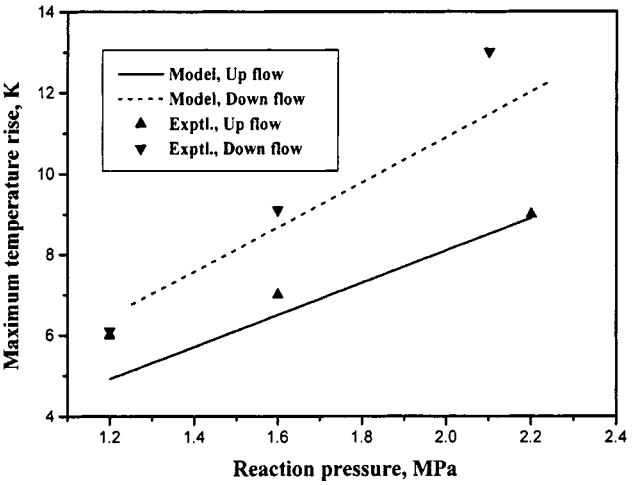

Figure 14. Effect of hydrogen pressure on temperature rise in trickle-bed and upflow modes.

Reaction conditions: T = 373 K, inlet CDT = 0.82 kmol/m^3; $U_l = 1.2\times10^{-3}$ m/s; $U_g = 3.9\times10^{-3}$ m/s.

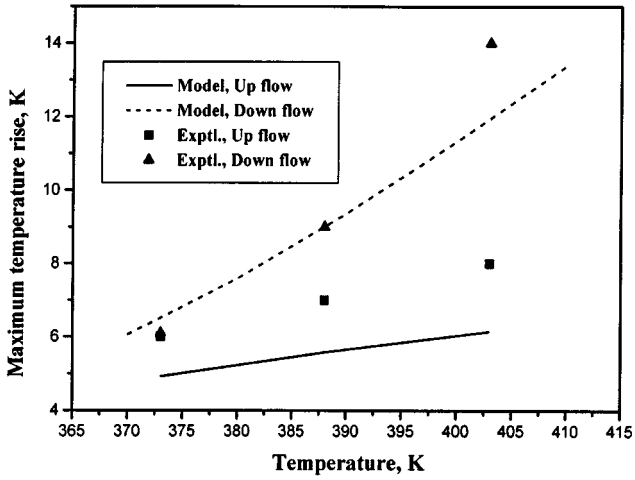

Figure 16. Effect of inlet temperature on temperature rise in trickle-bed and upflow modes.

Reaction conditions: inlet CDT = 0.82 kmol/m^3; P_H = 1.2 Mpa; $U_l = 1.2\times10^{-3}$ m/s; $U_g = 3.9\ \text{x}10^{-3}$ m/s.

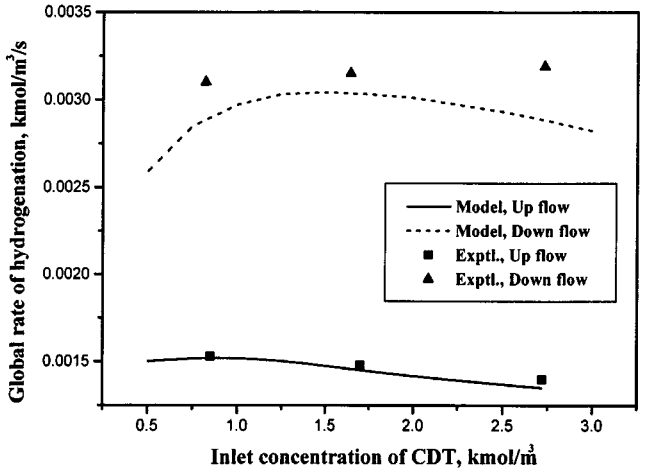

Figure 17. Effect of inlet CDT concentration on global rate of hydrogenation in trickle-bed and upflow modes.

Reaction conditions: $T = 373$ K; $P_H = 1.2$ MPa; $U_l = 1.2 \times 10^{-3}$ m/s; $U_g = 3.9 \times 10^{-3}$ m/s.

and inefficient external as well as internal wetting of catalyst. (2) The temperature rise is lower for the upflow mode, which also results in a lower rate, but can be a useful tool for temperature control. (3) The selectivity of CDE in relation to CDA was higher in the upflow mode, but when compared with all the products formed, it was higher in the downflow mode. The selectivity behavior at different conditions observed experimentally was also found to agree with the model predictions.

Acknowledgments

The authors thank IFCPAR (Indo-French Center for the Promotion of Advanced Research) for financial support of this work. One of the authors (S.P.M.) wishes to thank the Council of Scientific and Industrial Research (CSIR), India, for providing him a research fellowship.

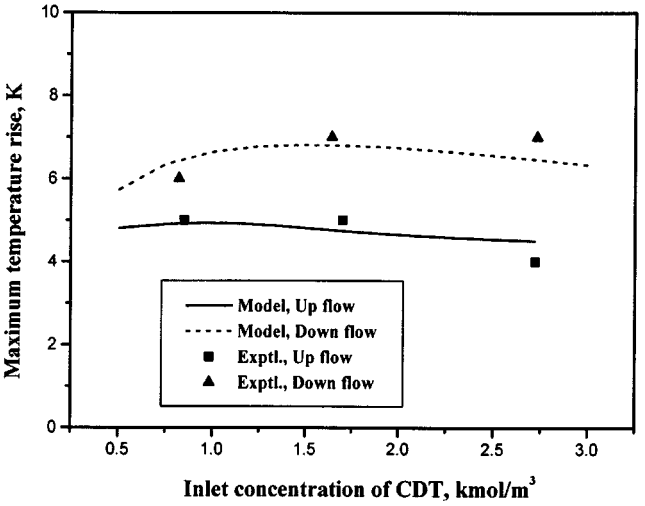

Figure 18. Effect of inlet CDT concentration on temperature rise in upflow and downflow reactors.

Reaction conditions: $T = 373$ K; $P_H = 1.2$ MPa; $U_l = 1.2 \times 10^{-3}$ m/s; $U_g = 3.9 \times 10^{-3}$ m/s.

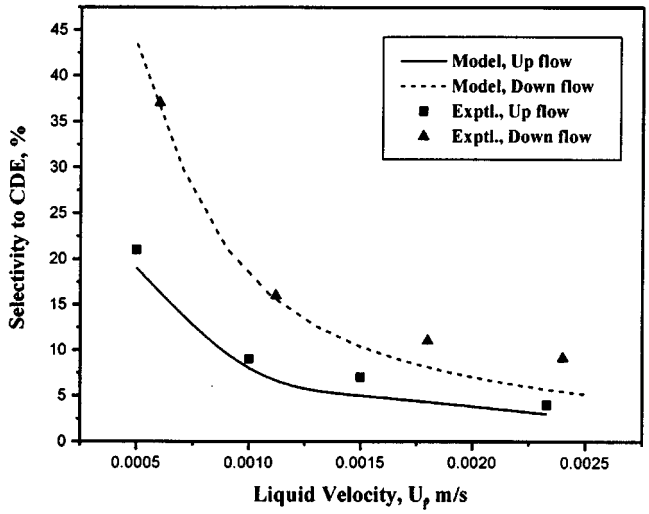

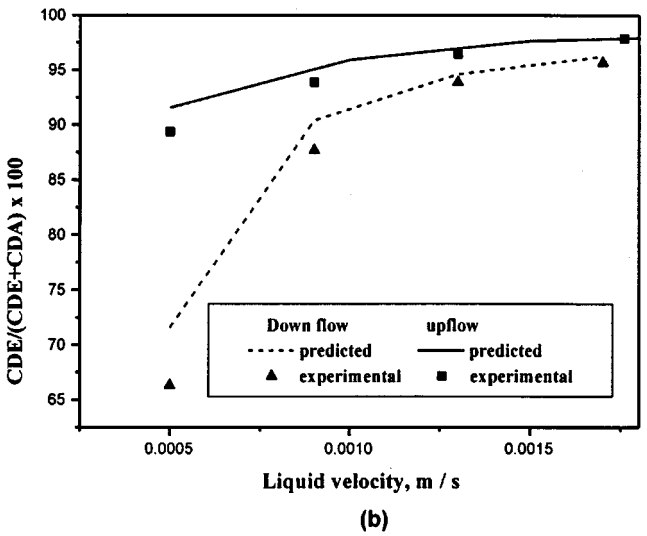

Figure 19. Effect of liquid velocity on selectivity for upflow and downflow reactors

Reaction conditions: $T = 373$ K; inlet CDT = 0.82 kmol/m^3; $P_H = 1.2$ MPa; $U_g = 3.9 \times 10^{-3}$ m/s.

Notation

a_B = gas–liquid interfacial area, m^2/m^3
a_l = dimensionless concentration of hydrogen in liquid phase, (A_l/A^*)
a_s = dimensionless concentration of hydrogen on the catalyst surface, (A_s/A^*)
a_p = external surface area of the pellet, $[6\ (1-\epsilon_B)/d_p]$, m^{-1}
a_t = packing external surface area per unit volume of reactor $[S_{ex}\ (1-\epsilon_B)/V_R]$, m^{-1}
a_w = catalyst area wetted, m^{-1}
A_l = concentration of hydrogen in liquid phase, kmol/m^3
A_s = concentration of hydrogen on the catalyst surface, kmol/m^3
A^* = concentration of hydrogen in equilibrium with liquid, kmol/m^3

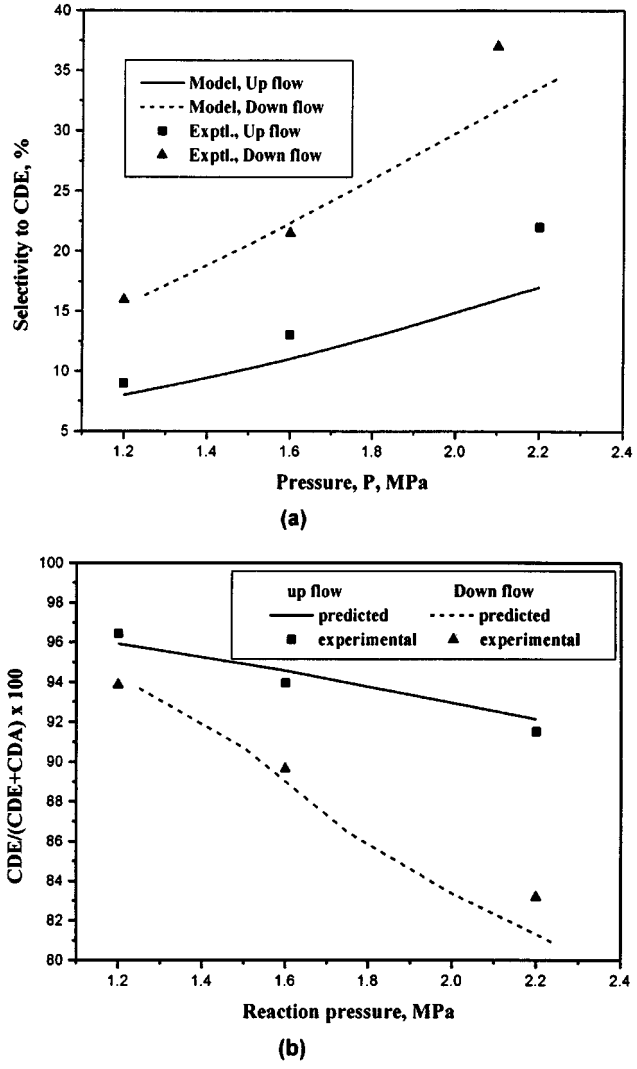

Figure 20. Effect of hydrogen pressure on selectivity for upflow and downflow reactors.

Reaction conditions: T = 373 K; inlet CDT = 0.82 kmol/m^3; $U_l = 1.2\times10^{-3}$ m/s; $U_g = 3.9\times10^{-3}$ m/s.

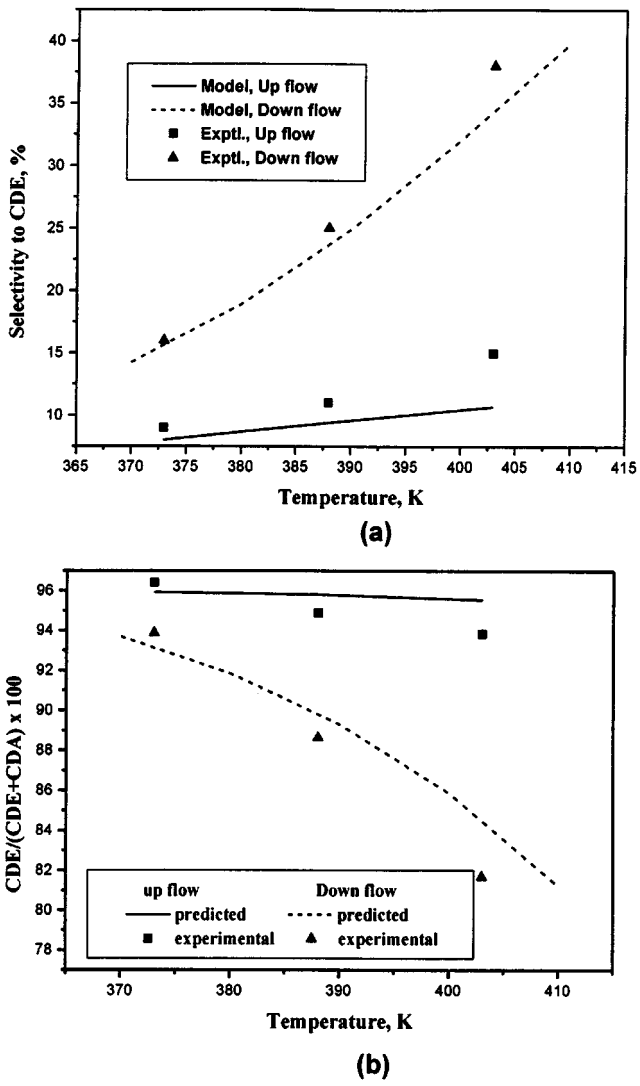

Figure 21. Effect of inlet temperature on selectivity of CDE for upflow and downflow reactors.

Reaction conditions: inlet CDT = 0.82 kmol/m^3; P_H = 1.2 MPa; $U_l = 1.2\times10^{-3}$ m/s; U_g = 3.9 x10^{-3} m/s.

b_l = dimensionless concentration of CDT in liquid phase, (B_l/B_{li})
B_l = concentration of CDT in liquid phase, kmol/m^3
B_{li} = initial concentration of CDT in liquid phase, kmol/m^3
c_l = dimensionless concentration of CDD in liquid phase, (C_l/B_{li})
C_l = concentration of CDD in liquid phase, kmol/m^3
C_{pl} = heat capacity of liquid, kJ/K/kg
C_{pg} = heat capacity of gas, kJ/K/kg
D_e = effective diffusivity, m^2/s
D_M = molecular diffusivity, m^2/s
d_p = particle diameter, m
d_T = reactor diameter, m
e_l = dimensionless concentration of CDE in liquid phase, (E_l/B_{li})
E_l = concentration of CDE in liquid phase, kmol/m^3
E_i = activation energy for hydrogenation step i, kJ/mol
f_d = fraction of catalyst wetted by the dynamic liquid
f_s = fraction of catalyst wetted by the stagnant liquid
f_w = wetted fraction
H_e = Henri's constant of solubility, kmol/m^3/atm
h_w = overall heat-transfer coefficient, kJ/m^2/K/s
k_1 to k_4 = reaction rate constants, (m^3/ kg) (m^3/kmol) s^{-1}
k_{21} = dimensionless rate constant (k_2/k_1)
k_{31} = dimensionless rate constant (k_3/k_1)
k_{41} = dimensionless rate constant (k_4/k_1)
k_b, k_c, k_e = dimensionless equilibrium constants ($k_b = K_{Bli}$; $k_c = K_C B_{li}$; $k_e = K_E B_{li}$)
k_s = liquid–solid mass-transfer coefficient, m·s^{-1}
k_{gs} = gas–particle mass transfer coefficient, m·s^{-1}
K_B,K_C, K_E = equilibrium constants, m^3/kmol
$k_l a_B$ = gas–liquid mass-transfer coefficient, s^{-1}
K_{ex} = exchange coefficient between dynamic and stagnant liquid, s^{-1}
L = reactor length, m
L_m = superficial liquid-mass velocity, kg/m^2/s
N_d = Nusselt number for liquid phase in the dynamic zone
N_s = Nusselt number for liquid phase in the stagnant zone
N_g = Nusselt number for gas phase
p_l = dimensionless concentration of CDA in liquid phase (P_l/B_{li})
P_l = concentration of CDA in liquid phase, kmol/m^3

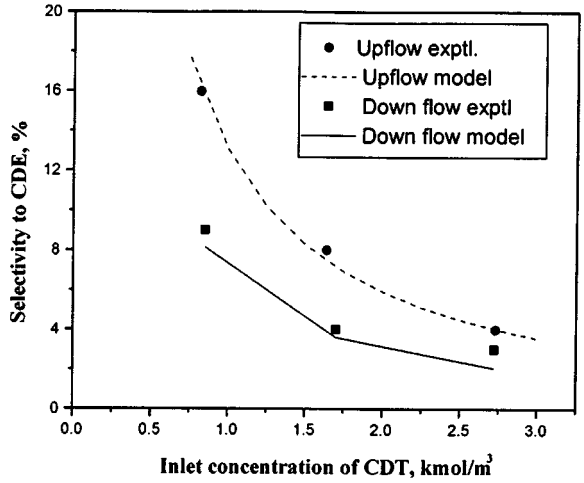

(a)

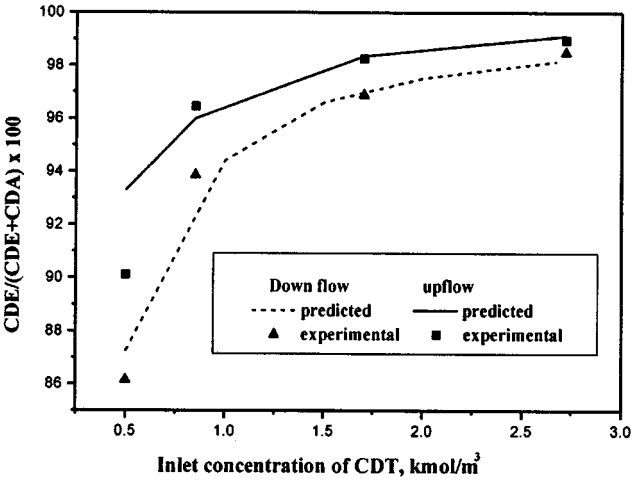

(b)

Figure 22. Effect of inlet CDT concentration on selectivity of CDE for upflow and downflow reactors.

Reaction conditions: $T = 373$ K; $P_H = 1.2$ MPa; $U_l = 1.2 \times 10^{-3}$ m/s; $U_g = 3.9 \times 10^{-3}$ m/s.

P_v = vapor pressure of solvent, mm Hg (as defined by Eq. 18)
P_r = Prandtl number of liquid phase ($C_{pl}\,\mu_l/\lambda_{\text{eff}}$)
q_B = stoichiometric ratio (3 B_{li}/A^*)
r_1 to r_3 = reaction rate for individual hydrogenation steps, kmol/m^3/s
R = radius of the pellet, m
R_a = global rate of hydrogenation, kmol/m^3/s
R_g = universal gas constant, kJ/kmol/K
Re_l = Reynolds number for liquid phase
S_{ex} = external surface area of the catalyst pellet, m^2
T_o = inlet temperature, K
T_b = bed temperature, K
T_W = wall temperature, K
U_W = bed-to-wall heat-transfer coefficient, kJ / m^2 / K / s
U_g = gas velocity, m/s
U_l = liquid velocity, m/s
V_R = reactor volume, m^3
w = catalyst loading kg/m^3
We_l = Weber number for liquid (L_m^2 / ($\sigma_l\,\rho_l\,a_t$)
z = dimensionless reactor length

Greek letters

α_{gl} = dimensionless gas–liquid mass-transfer coefficient
α_{ls} = dimensionless liquid–solid mass-transfer coefficient
α_r = dimensionless reaction rate constant
α_s = dimensionless exchange coefficient
β_1 = thermicity parameter
β_2 = dimensionless heat-transfer parameter
δ_{gl} = two-phase pressure drop, N/m^2
χ = parameter defined by Eq. 16
ΔH = heat of reaction, kJ/mol
ϵ = porosity of catalyst
ϵ_b = bed voidage
ϵ_l, ϵ_d, ϵ_s = liquid holdup, total, dynamic, and stagnant
η_c = overall catalytic effectiveness factor
η_d, η_s, η_g = catalytic effectiveness factors for dynamic, stagnant, and dry zones
θ = dimensionless temperature
θ_b = dimensionless bed temperature
θ_w = dimensionless wall temperature
μ_l = viscosity of liquid
ρ_l = density of liquid, kg/m^3
ρ_g = density of gas, kg/m^3
ρ_p = density of catalyst particle, kg/m^3
σ_l = surface tension, N/m
τ = tortuosity factor
ϕ = Thiele parameter

Subscripts

d = dynamic zone
g = dry zone
s = stagnant zone

Literature Cited

Al-Dahhan, M. H., and M. P. Dudukovic, "Catalyst Bed Dilution for Improving Catalyst Wetting in Laboratory Trickle Bed Reactors," *AIChE J.*, **42**, 2595 (1996).

Al-Dahhan, M. H., F. Larachi, M. P. Dudukovic, and A. Laurent, "High-Pressure Trickle-Bed Reactors: A Review," *Ind. Eng. Chem. Res.*, **36**, 3292 (1997).

Baldi, G., *Multiphase Chemical Reactors*, Vol. II, *Design Methods*, A. E. Rodrigues, J. M. Cole, and N. M. Sweed, eds., Sithoff and Noorldhoff, Alphen aan den Rijn, The Netherlands, p. 307 (1981).

Benaissa, M., G. C. Le Roux, X. Joulia, R. V. Chaudhari, and H. Delmas, "Kinetic Modeling of the Hydrogenation of the Hydrogenation of 1,5,9-Cyclododecatriene on Pd/Al_2O_3 Catalyst Including Isomerization," *Ind. Eng. Chem. Res.*, **35**, 2091 (1996).

Bergault, I., M. V. Rajashekharam, R. V. Chaudhari, D. Schweich, and H. Delmas, "Modelling of Comparison of Acetophenone Hydrogenation in Trickle-Bed and Slurry Airlift Reactors," *Chem. Eng. Sci.*, **52**, 21/22, 4033 (1997).

Bischoff, K. B., "Effectiveness Factors for General Reaction Rate Forms," *AIChE J.*, **11**, 351 (1965).

Brahme, P. H., R. V Chaudhari, and P. A Ramachandran, "Modelling of Hydrogenation of Glucose in a Continuous Slurry Reactor," *Ind. Eng. Chem. Proc. Des. Dev.*, **23**, 857 (1984).

Dassori, C. G., "Three Phase Reactor Modeling with Significant Back Mixing in the Liquid Phase Using Modified Cell Model (MCM)," *Chem. Eng. Sci.*, **22**(Suppl.), S679 (1998).

DeWind, M., F. L. Plantenga, J. J. L. Heinerman, and H. W. Homanfree, "Upflow Versus Downflow Testing of Hydrotreating Catalysts," *Appl. Catal.*, **43**, 239 (1988).

Dudukovic, M. P., F Larachi, and P. L. Mills, "Multiphase Reactors —Revisited, Chem. Eng. Sci., **54**, 1975 (1999).

Fukushima, S., and K. Kusaka, "Liquid-Phase Volumetric Mass Transfer Coefficient and Boundary of Hydrodynamics Flow Regime in Packed Column with Co Current Downward Flow," *J. Chem. Eng. Jpn.*, **10**, 468 (1977).

Goto, S., K. Mabuchi, "Oxidation of Ethanol in Gas-Liquid Cocurrent Upflow and Downflow Reactors," *Can. J. Chem. Eng.*, **62**, 865 (1984).
Hanika, J., K. Sporka, V. Ruzicka, and R. Pistek, "Dynamic Behaviour of an Adiabatic Trickle Bed Reactor," *Chem. Eng. Sci.*, **32**, 525 (1977).
Herrmann, U., and G. Emig, "Liquid Phase Hydrogenation of Maleic Anhydride to 1-4, Butanediol in a Packed Bubble Column Reactor," *Ind. Eng. Chem. Res.*, **37**, 759 (1998).
Hochman, J. M., and E. Effron, "Two Phase Cocurrent Downflow in Packed Beds," *Ind. Eng. Chem. Fundam.*, **8**, 63 (1969).
Jaganathan, R., R. V. Gholap, P. H. Brahme, and R. V. Chaudhari, "Performance of a Continuous Bubble Column Slurry Reactor for Hydrogenation of Butynediol, *Proc. of ICREC 2*, Vol. II, NCL, India, p. 141 (1987).
Jaganathan, R., V. G. Ghugikar, R. V. Gholap, R. V. Chaudjari, and P. L. Mills, "Catalytic Hydrogenation of *p*-Nitrocumene in a Slurry Reactor," *Ind. Eng. Chem. Res.*, **38**, 4634 (1999).
Julcour, C., R. Jaganathan, R. V. Chaudhari, A. M. Wilhelm, and H. Delmas, "Selective Hydrogenation of 1,5,9-Cyclododecatriene in Upflow and Downflow Fixed Bed Reactors, Experimental Observations and Modeling," *Chem. Eng. Sci.*, **56**, 557 (2001).
Khadilkar, M. R., Y. X. Wu, M. H. Al-Dahhan, and M. P. Dudukovic, "Comparison of Trickle Bed and Upflow Reactor Performance at High Pressure: Model Prediction and Experimental Observations," *Chem. Eng. Sci.*, **51**, 2139 (1996).
Khadilkar, M. R., Y. Jiang, M. Al-Dahhan, M. P. Dudukovic, S. K. Chou, G. Ahmed, and R. Kahney, "Investigations of a Complex Reaction Network: I Experiments in a High-Pressure Trickle Bed Reactor," *AIChE J.*, **44**, 912 (1998).
Leung, P., C. Zorrilla, F. Recasens, and J. M. Smith, "Hydration of Isobutene in Liquid-Full and Trickle Bed Reactors," *AIChE J.*, **32**, 1839 (1986).
Mills, P. L., E. G. Beaudry, and M. P. Dudukovic, "Comparison and Prediction of Reactor Performance for Packed Beds with Two-Phase Flow: Downflow, Upflow and Countercurrent Flow," *Inst. Chem. Eng. Symp. Ser.*, **87**, 527 (1984).
Mills, P. L., and M. P. Dudukovic, "Evaluation of Liquid-Solid Contacting in Trickle Bed Reactors by Tracer Methods," *AIChE J.*, **27**, 893 (1981).
Mills P. L., and R. V. Chaudhari, "Multiphase Catalytic Reactor Engineering and Design for Pharmaceuticals and Fine Chemicals," *Catal. Today*, **37**, 367 (1997).
Mochizuki, S. and T. Matsui, "Selective Hydrogenation and Mass Transfer in a Fixed Bed Catalytic Reactor with Gas-Liquid Concurrent Upflow," *AIChE J.*, **22**, 904 (1976).
Ragaini, V. and C. Tine, "Upflow Reactor for the Selective Hydrogenation of Pyrolysis Gasoline: Comparative Study with Respect to Downflow," *Appl. Catal.*, **10**, 43 (1984).
Rajashekharam, M. V., D. D. Nikalje, R. Jaganathan, and R. V. Chaudhari, "Hydrogenation of 2,4-Dinitrotoluene Using Pd/Al_2O_3 Catalyst in a Slurry Reactor: A Molecular Level Approach to Kinetic Modelling and Nonsiothermal Effects," *Ind. Eng. Chem. Res.*, **36** , 592 (1997).
Rajashekharam, M. V., R. Jaganathan, and R. V. Chaudhari, "A Trickle-Bed Reactor Model for Hydrogenation of 2,4 Dinitrotoluene: Experimental Verification," *Chem. Eng. Sci.*,**53**, 4, 787 (1998).
Ramachandran, P. A. and R. V. Chaudhari, "Three Phase Catalytic Reactors," Gorden & Breach, New York (1983).
Reiss, L. P., "Cocurrent Gas-Liquid Contacting in Packed Columns," *Ind. Eng. Chem. Proc. Des. Dev.*, **6**, 486 (1967).
Sato, Y., T. Hiros, F. Takahashi, and M. Toda, "Pressure Loss and Liquid Holdup in Packed Bed Reactor with Cocurrent Gas-Liquid Flow," *J. Chem. Eng. Jpn.*, **6**, 147 (1973).
Satterfield, C. N., M. W. Vab Eek, and G. S. Bliss, "Liquid-Solid Mass Transfer in Packed Beds with Down Flow Cocurrent Gas-Liquid Flow," *AIChE J.*, **24**, 709 (1978).
Specchia, V., G. Baldi, and A. Gianetto, "Solid-Liquid Mass Transfer in Cocurrent Two-Phase Flow Through Packed Beds," *Ind. Eng. Chem. Proc. Des. Dev.*, **17**, 362 (1978).
Steigel, G. J., and Y. T. Shah, "Backmixing and Liquid Holdup in Gas-Liquid Cocurrent Upflow Packed Column," *Ind. Eng. Chem. Proc. Des. Dev.*, **16**, 37 (1977).
Stephen, H., and I. Stephen, *Solubilities of Inorganic and Organic Compounds*, Part 1, Vol. 1, Pergamon Press, London, p. 543 (1963).
Stuber, F., M. Benaissa, and H. Delmas, "Partial Hydrogenation of 1,5,9-Cyclododecatriene in Three Phase Catalytic Reactors," *Catal. Today*, **24**, 95 (1995)
Trambouze, P., "Multiphase Catalytic Reactors in the Oil Industry: an Introduction," *Rev. Inst. Fr. Pet.*, **46**, 433 (1991).
Turpin, J. L., and R. L. Huntington, "Prediction of Pressure Drop for Two Phase, Two Component Cocurrent Flow in Packed Beds," *AIChE J.*, **13**, 1196 (1967).
van Gelder, K. B., J. K. Damhof, P. J. Krouenga, and K. R. Westertrep, "Three Phase Packed Bed Reactor with an Evaporating Solvent I: Experimental: The Hydrogenation of 2,4,6-Trinitrotoluene in Methanol," *Chem. Eng. Sci.*, **45**, 3159 (1990a).
van Gelder, K. B., P. C. Borman, R. E. Weenink, and K. R. Westertrep, "Three Phase Packed Bed Reactor with an Evaporating Solvent: II. Modelling the Reactor," *Chem. Eng. Sci.*, **45**, 3171 (1990b).
Wilke, C. R., and P. Chang, "Correlation of Diffusion Coefficients in Dilute Solutions," *AIChE J.*, **1**, 264 (1955).
Wu, Y., M. R. Khadilkar, M. H. Al-Dahhan, and M. P. Dudukovic, "Comparison of Upflow and Downflow Two-Phase Flow Packed Bed Reactors with and Without Fines: Experimental Observation," *Ind. Chem. Eng. Res.*, **35**, 397 (1996).

Manuscript received Dec. 19, 2000, and revision received May 17, 2001.